Stick-Release Pattern in Stretching Single Condensed Polyelectrolyte Toroids

Paul Cárdenas-Lizana and Pai-Yi Hsiao*

Department of Engineering and System Science, National Tsing Hua University, Hsinchu, Taiwan 300, R.O.C.

Received September 17, 2008
Revised Manuscript Received February 26, 2009

There are continually strong demands in understanding the properties of DNA molecules because of their broad implications in biology and the benefits in gene therapy.[1] Owing to the progress of nanotechnology, researchers are now allowed to investigate the elastic response of DNA under the action of an external force, at the level of single molecules.[2] When a DNA molecule was stretched, different kinds of force-extension curve (FEC) have been observed,[3−5] depending on the multivalent counterion concentration, C, in the solution. For C staying outside the region bounded by the condensation threshold C_c and the decondensation threshold C_d ($C_c < C_d$), DNA molecules are in a coil state and FEC is basically described by the Marko−Siggia formula derived from the wormlike chain (WLC) model.[6] For C inside the region, the DNAs are collapsed into globule of ordered structure and the preferable structure is toroid.[7] At this moment, FEC shows *plateau force* while $C \sim C_c$, or *stick-release pattern* while C is close to C_0, where C_0 is the salt concentration at which the effective chain charge is neutralized by the multivalent counterions.[8] For the plateau force, the elastic response is constant over a wide range of chain extension and its value is larger than the prediction of the WLC model, whereas for the stick-release pattern, the force is periodic and piecewisely described by the Marko−Siggia formula.[3,5]

It was suggested that the plateau force is derived from the fact that the ratio of the extension to the effective chain contour length is a constant and thus produces a constant force according to the Marko−Siggia formula.[9] To explain the stick-release pattern, two models have been proposed. The first model[9,10] is based upon the observation of the *rings-on-a-string* structure of a long DNA chain. The formation of this gripping pattern could be a consequence of the abrupt breaking of one ring into several under the stretching of an external force. Elastic response between ring breakings is determined by the coil part of the chain and follows the WLC model. The second model,[5,11] on the other hand, attributes this phenomenon to a result of the loop-by-loop unfolding of a toroidal DNA condensate under stretching, because a pronounced quantization in the DNA release length of about 300nm has been demonstrated, which correlates exactly with the periphery length of a typical DNA toroid of size $R \simeq 50$ nm. Nevertheless, a concrete evidence is still missing and researchers cannot make a conclusive connection of the stick-release pattern with the second model yet.

Recently, the pathway of unwrapping a spool of DNA chain helically coiled onto a histone protein has been studied by theorists to investigate the stability and dynamics of nucleosomes under tension.[12] They pointed out the similarity between two seemingly unrelated problems: unwrapping of nucleosomes and unfolding of DNA toroidal condensates, and predicted a catastrophic event for the two systems under tension: a sudden and quantized unraveling happened once a time for a DNA turn. This unwrapping pathway is difficult to be investigated by experiments and the information concerning the internal structure of toroidal DNA condensates under tension is still not complete. Therefore, in this study, we conduct computer simulations to study the elastic response of a toroidal polyelectrolyte (PE) condensate and investigate structural variation and unfolding dynamics of chain under tension. We focus on the case that the amount of multivalent counterions is in charge equivalence with the PE chain. This choice gives us the most chance to observe the stick-release pattern. There have been simulation works devoting to the study of PE chains under tension.[11,13,14] However, in most of the works, the chains were flexible and condensed into disordered structures either by compacting potentials or by monovalent counterions with a ultrastrong Coulomb coupling. Our work here, on the contrary, deals with a more realistic situation in an ambient condition where the chain is semiflexible, collapsed by multivalent counterions into a toroid. This kind of study is still scarce,[15] and it involves nonlinear and nonequilibrium effects coming from the arrangement of ions, the long-range Coulomb interaction, and the pulling speed.

Our system contains a single chain and many counterions. The chain is composed of $N_m = 512$ monomers, each of which carries a negative unit charge, $-e$. The counterions are tetravalent and the number of the counterions is 128. The excluded volume of the monomers and the counterions is modeled by the Lennard-Jones potential $\varepsilon_{LJ}[2(\sigma/r)^6 - 1]^2$ truncated at the minimum. We assumed an identical ε_{LJ} for the monomers and counterions but different diameter σ. The diameter of the counterions σ_c is half of that of the monomers σ_m. In the following text, we use ε_{LJ} and σ_c as the units of energy and length, respectively. Two consecutive monomers on the chain are connected by a bond of length b via the harmonic potential $k_b(b - b_0)^2$ with $k_b = 100$ and $b_0 = 1.1$. The chain stiffness is described by an angle potential $k_2(\theta - \theta_0)^2 + k_4(\theta - \theta_0)^4$ with $k_2 = 5$, $k_4 = 200$ and $\theta_0 = \pi$, where θ is the angle between two adjacent bonds on the chain. Coulomb interaction is expressed by $\lambda_B k_B T z_i z_j / r$ where r is the separation distance of two particles of valences z_i and z_j, and λ_B is the Bjerrum length. We set $\lambda_B = 4.68$ and the temperature $k_B T = 1.2$. We assumed further that the bond potential and the angle potential have already incorporated the effect of nonbonded interactions along the chain, including the excluded volume interaction and Coulomb interaction. Therefore, the nonbonded interactions are deactivated for pairs of monomers separated by less than three bonds on the chain. This kind of setup has been used in simulations. The advantage of this setup is that the bond and the angle potentials given here have been the *entire* potentials without need to take into account further the nonbonded interactions between the monomers. Please notice that the deactivation of Coulomb interaction locally on the chain will not violate the requirement of charge neutrality because it is a global property of a system and the total charge is always zero. The system is placed in a rectangular box of size $620 \times 91 \times 91$ and periodic boundary condition is applied. The technique of PPPM Ewald sum is employed to calculate the Coulomb interaction. We performed Langevin dynamics simulations[16] with the friction coefficient ζ setting to $2\tau^{-1}$ and $1\tau^{-1}$ for the monomers and the counterions, respectively, where $\tau = \sigma_c\sqrt{(m/\varepsilon_{LJ})}$ is the time unit and m is the particle mass. Stevens has used a similar model[17]

* Corresponding author. E-mail: pyhsiao@ess.nthu.edu.tw

10.1021/ma802120b CCC: $40.75
Published on Web 03/20/2009

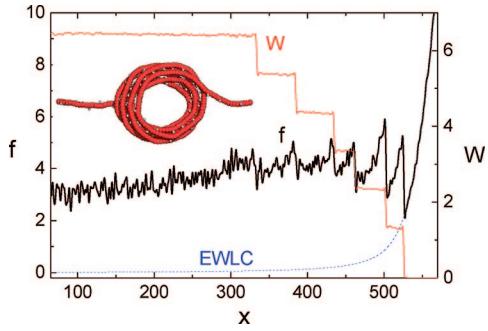

Figure 1. Force f vs extension x (thick solid curve). The dashed line is the fitting curve for $x \geq 526$ by the EWLC model. W is plotted in solid curve and the value is read from the right axis of ordinate. The inset is a snapshot of the chain before stretching.

and shown that a PE chain can collapse into a toroid due to the condensation of tetravalent counterions. Since the line charge density matches that of a double-stranded DNA (dsDNA) and the size of monomer matches the size of a phosphate group, our model can be used to understand the system of DNA condensed into a toroid. We remark that the persistence length in our model is 1 order of magnitude shorter than dsDNA. The reason for this setup is to allow the formation of a toroid in a short chain length; thus the simulations become feasible under limited computing resources.

The initial configuration of chain is a circular helix with its central line lying on the x axis. This configuration is used to favor the formation of a toroid. Other structures, such as cigar or racket shapes, sometimes appear in the simulations.[17,18] All these structures have been observed in experiments of DNA condensation and people believe that toroid is the most stable structure.[7] Since different condensed structure could produce different FEC under tension, in this study we focus on the case of chains collapsing into toroids. The two chain ends are guided by a spring force toward two points on the x-axis with separation distance equal to 60. After reaching a stable state, most of the chains form *rod*−*toroid*−*rod* structure as shown in the inset of Figure 1. Since chain ends are constrained, knots will not appear on the chain. We have chosen different radii and pitches of helix as our initial configurations and verified that the size of the generated toroid is independent of these choices. The toroid size is defined by two radii, the minor radius r_0 and the major radius R_0. The previous one is the radius of the annular tube of the toroid and the latter is the radius measured from the toroid center to the center of the annular tube. These two radii determine the gyration tensor of a toroid with the three eigenvalues equal to $r_0^2/4$, $(4R_0^2 + 3r_0^2)/8$, and $(4R_0^2 + 3r_0^2)/8$. The gyration tensor of a set of N particles can be calculated by simulations according to the equation $T_{\alpha\beta} = \sum_{i=1}^{N} (\vec{r}_i - \vec{r}_{cm})_\alpha (\vec{r}_i - \vec{r}_{cm})_\beta / N$ where $\vec{r}_{cm}$is the center of mass of the set of particles and the subscripts α and β denote the three Cartesian components. We calculated the gyration tensor of the toroid on the chain and estimated r_0 and R_0 from the three eigenvalues λ_i (i = 1,2,3). The results are r_0 = 3.60(1) and R_0 = 12.3(1). It is known that a ring structure ($r_0 \ll R_0$) can be characterized by a quantity, called *asphericity*, defined as $A = \sum_{i=1}^{3}\sum_{j=1}^{3}(\lambda_i - \lambda_j)^2/(2\sum_{i=1}^{3}\lambda_i)^2$, with its value equal to 0.25. Since our toroid has a finite r_0, A is smaller than 0.25 and takes a value of 0.235(1). The winding number W is another important quantity to describe the status of a toroid, which counts the number of turns winding around the toroid central axis. Our toroidal condensates have W = 6.5 before stretching. The decimal 0.5 in W reflects the fact that the two chain ends stay on the opposite sides of the toroid.

We fixed one end of the condensed PE chains and pulled the other end outward along the x-axis using a spring force with constant pulling speed v = 0.0005. Since unfolding of a condensed PE is a nonequilibrium process, it is delicate to choose the pulling speed.[11,14] We have verified that significant nonequilibrium effect is detected only when the pulling speed excesses the characteristic speed, $v_s = R_0/\tau_R \sim 0.002$, estimated by the Rouse relaxation time τ_R. Our choice of v is slow enough to minimize the dependence of FEC on the pulling speed, which essentially probes the elastic response of PEs in the limit of zero pulling speed.[14] Nevertheless, it does not mean that our chains reach equilibrium for every stretched distance. To study it, one needs to perform equilibrium simulations with the chain ends fixed on every stretched distance. However, this sort of approach demands much more computing resources. For practical purpose to understand the stick-release pattern of a toroidal DNA condensate under tension, we decided to follow the arguments given by Lee and Thirumalai[14] that the nonequilibrium method with a small pulling speed can be a good approach, sufficient enough to study the problems of the elasticity, the internal structure, and the dynamics.

We prepared 20 independent toroids and performed stretching process. A typical FEC obtained in our simulations is shown in Figure 1. The extension x is the distance between two chain ends. The data have been passed through a low-pass filter to attenuate the high-frequency noise. We have verified that the filter does not modify the content of the force curve. The FEC shows approximately a plateau force up to $x \approx 270$. After that, the force increases and then decreases abruptly with extension. This tooth-like structure repeatedly appears in the FEC and becomes shaper and sharper as the extension increases. This is so-called stick-release pattern, which has been experimentally reported.[3,5] We plot in the same figure the winding number W. We see that W is a downstairs function and the height of each stairstep is equal to one. It shows that the toroidal PE looses one loop, followed by one loop, under stretching. The results support the picture of Murayama et al.[5] The dynamics that one loop breaks into several was not observed in this study. Moreover, we observed that the sawteeth in FEC appear coherently with the steps of W. Each sawtooth corresponds exactly to one step in W. It demonstrates that the stick-release pattern is a consequence of the loop-by-loop unfolding of the condensed PE toroid, and confirms the theoretical picture of stepwise unwinding of PE under stretching.[19]

In the final stage of the stretching ($x > 525$), f increases largely and the elastic response is similar to the WLC model. Since our chain is extensible, we fitted these data by the modified Marko−Siggia formula[20] derived from the extensible WLC (EWLC) model,

$$\frac{fP}{k_BT} = \frac{x}{L} + \frac{1}{4(1 - x/L + f/K)^2} - \frac{1}{4} - \frac{f}{K} \qquad (1)$$

where L is the contour length, P is the persistence length, and K is the elastic modulus. We obtained L = 559.7, P = 25.2 and K = 230.2 by fitting in the region $x > 525$. The fitting curve f_{EWLC}, plotted in dashed line in Figure 1, matches well with the FEC in this region. The fitting values are consistent with the theoretical ones, $L = (N_m - 1)b_0$ = 562.1 and $K = 2k_bb_0$ = 220. It is known that P is a sum of two contributions; one is the intrinsic persistence length P_0 originating from the chain bare stiffness, and the other is the electrostatic persistence length P_e owing to the Coulomb repulsion between monomers on the chain. In this study, we calculated P_0 by equating the bending

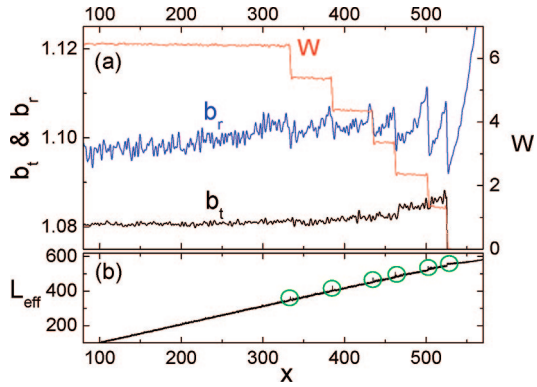

Figure 2. (a) b_t and b_r. (b) L_{eff} as a function of x. W is plotted in the figure (a) to indicate the occurrence of the loop-by-loop unfolding.

energy E_{bend} to $k_BT/2$ for a chain segment of length P_0 with the bending angle equal to 1 rad. E_{bend} is equal to $(k_2(b_0/P_0)^2 + k_4(b_0/P_0)^4) \times (P_0/b_0)$ because there are P_0/b monomers on the chain segment and the bond angle θ at each monomer is $\pi - (b_0/P_0)$ in average. By solving this equation, we have $P_0 = 12.2$, which gives an estimation of P_e equal to $P - P_0 = 13.0$. It is worth noticing that P_0 obtained here is approximately equal to the major radius R_0 of the toroidal condensate before stretching. This is a result of charge neutralization. The condensed tetravalent counterions neutralize the chain charge and therefore, the electrostatics does not play a major role in determination of the toroid size. At this moment, P_e is roughly zero as shown in the previous study of flexible chains.[21] So the major radius relates directly the intrinsic persistence length of a PE.

We calculated the excess work for the toroidal condensate $\Delta W = \int_{60}^{525}(f - f_{EWLC})\,dx$, and found $\Delta W = 1658$. Therefore, the condensation energy is 3.47 per monomer (because the toroid part of the chain contains 478 monomers before stretching). This energy is mainly determined by the energy needed to break an *electrostatic binding* between a condensed tetravalent counterion and a monomer, which reads as $|\lambda_B k_B T(+4)(-1)/1.5| = 14.98$ or equivalently 3.74 per monomer. This finding suggests an electrostatic origin for the PE chain condensation.

The condensed chain preserves the rod−toroid−rod structure in most of the time during stretching. In order to understand more deeply the elastic response, we calculated the average bond length on the toroid part, b_t, and on the rod part, b_r, of the chain. The results are presented in Figure 2a. We found that b_t stays roughly a constant up to $x \simeq 450$, and the value is 1.08. This value is smaller than the equilibrium value $b_0 = 1.1$ of a bond, obviously due to the condensation of the tetravalent counterions which tightly bind middle part of the chain to form a toroidal structure. It is this tight binding which makes shorter the bond length b_t. Since the toroid part consists of several loops, the effective elastic modulus on this part is very stiff. Therefore, the variation of b_t with the extension x is hardly seen. On the other hand, b_r on the rod part displays a sawtooth structure, coinciding with the FEC. This shows that the elastic response of the chain is mainly determined by the rod part. If f is strong enough to overcome the binding between the strands on the toroid, a loop is pulled out of it.

We also calculated the effective contour length of the chain L_{eff}, defined as the total length on the rod part plus the diameter of the toroid. The result is shown in Figure 2b. We see that L_{eff}, on the main trend, depends linearly on x, but, locally, shows a series of small peaks (enclosed inside circles in the figure). Each peak corresponds to the moment when a loop is pulled out of the toroid and the tension of the chain is suddenly released; consequently, f is sharply decreased and so is b_r. The linear dependence of L_{eff} tells us that x/L_{eff} is approximately constant during the pulling process, which suggests the existence of a reference force f_0. f_0 can be estimated by replacing x/L in eq 1 by x/L_{eff}. Since $x/L_{eff} \simeq 0.95$ in this study, f_0 is about 3.5.

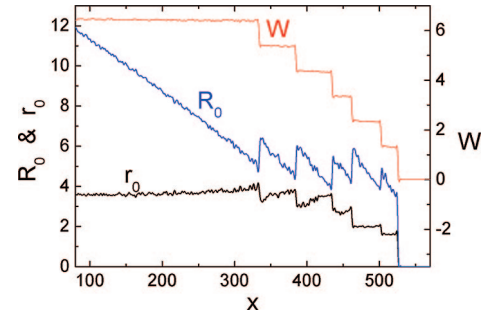

Figure 3. R_0, r_0, and W as a function of x.

We did find that the sawtooth structure of FEC oscillates around this reference force. These oscillations can be attributed to the fluctuations of L_{eff} (or b_r) due to the loop-by-loop unfolding of the chain. This phenomenon has been observed experimentally.[3−5] The observed reference force can be used to estimate x/L_{eff} in experiments by $x/L_{eff} = 1 - \sqrt{(k_BT/4Pf_0)}$,[6] which gives a typical value of 0.8 for DNA condensation, for e.g., by spermidine. This value is smaller than our simulation value 0.95. The discrepancy is due to the higher counterion valency and the smaller ion size used in this study, which leads to a stronger binding force between toroid loops than in the real experiments and hence, a larger f_0. Consequently, the condensation energy obtained here is higher than a typical value obtained by experiments, 0.08 to $0.3k_BT$ per base pair.[3−5]

We further investigated how the size of the toroid varies under stretching and the results are shown in Figure 3. We observed that the major radius R_0 decreases linearly until the release of the first loop. It abruptly increases at the moment when a loop is pulled out of the toroid, and then decreases with the extension. This behavior repeats many times and the final curve shows a sawtooth structure. For the minor radius r_0, we found that it is a downstairs function, decreasing simultaneously with W. When a loop is pulled out of the toroid, the number of the chain strands in the annular tube of the toroid decreases by one, and thus r_0 exhibits a discontinuous jump. These findings show that at the first stage of stretching, the toroid decreases its size constantly to some value. The size then oscillates around this value ($R_0 \simeq 5$ in this study) while the toroid starts to lose its loops, one by one, during the stretching process.

This structural transition has been approved by the snapshots, shown in Figure 4a. The snapshots clearly show that the diameter of the toroid first decreases to a critical value (pictures 1−3) and then keeps the value around this value for the rest of the loop releasing process (pictures 4−8). The breaking of the toroid into several loops (or toroids) is not observed in the simulations. We have verified that the other independent runs show the consistent elastic response. The W curves for these 20 independent runs are plotted in Figure 4b. The consistency of these curves confirms that the whole process is repeatable and the nonequilibrium effect has been minimized by our slow pulling speed. Therefore, the results can be used to understand the elastic response in a near-equilibrium condition. We, furthermore, calculated the mean value of x at which W decreases by a step. The results, W vs $\langle x \rangle$, are plotted in the inset of Figure 4b. We

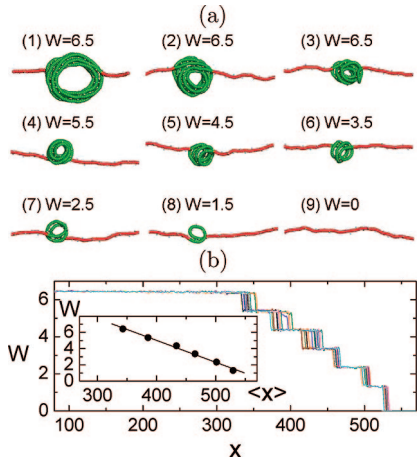

Figure 4. (a) Snapshots of simulations. The toroid part of the chain is colored in light (green) color. (b) W as a function of x for the 20 independent runs. The inset shows the averaged position $\langle x \rangle$ to occur a loss of one loop under stretching.

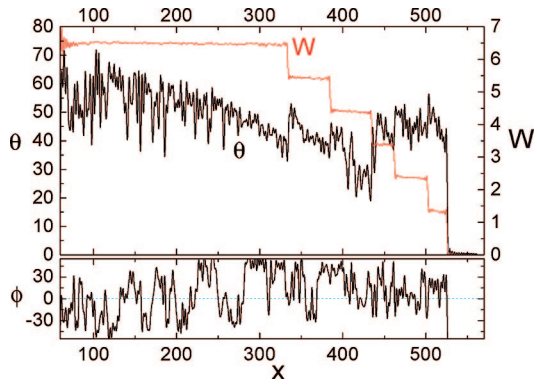

Figure 5. θ and ϕ, both in units of angles (deg), as a function of x. W is plotted to indicate the occurrence of the loop-by-loop unfolding.

see that $\langle x \rangle$ lies on a straight line, which demonstrates that the circumference of a loop is a constant. The slope of the line corresponds to a circumference $\Delta\langle x \rangle = 37.03$ per loop, or equivalently a circle of radius 5.9. This radius is consistent with the value of R_0 at the peaks of the sawteeth in Figure 3.

It is known that the persistence length of DNA is about 50 nm. Consequently, when DNA is collapsed into a toroid, the periphery length of the toroid is approximately 300 nm. Murayama et al. [5] have shown that the stick-release pattern has a periodicity characterized by a distance of 300 nm. This result supports the loop-by-loop unfolding of DNA, as do our simulations. Moreover, they found that the higher the salt concentration, the earlier the stick-release pattern happens in the stretching. Thus, the chain looses its first loop at a smaller extension position, according to our results. This can be understood by the phenomena of reentrant transition, in which a condensed DNA becomes less and less stable while the salt concentration is increased.[8,18] Because the loss of the first loop of toroid occurs at a larger R_0 at higher salt concentration, we predict that the periodicity of the stick-release pattern increases with salt concentration.

Finally, we studied the zenith angle θ, measured from the pulling-force direction to the normal direction of the toroid surface, to give insight of the unwrapping pathway of a toroidal condensate under tension. θ is plotted in Figure 5 as a function of x. We found that the chain was stretched from a starting zenith angle of about 65°. In the stretching process, θ showed piecewise decreasing behavior with x, happened coherently with the change of the winding number. Therefore, the toroid normal was pulled, over again, toward the force direction during the stretching and swung back to its early direction at each moment when the toroid released a loop. It is the sudden drop of the chain tension which restores the normal vector back to its early direction. We also calculated the azimuthal angle ϕ of the normal vector, plotted in Figure 5 too, which shows that the projection of the vector on the plane perpendicular to the pulling direction fluctuated around a reference direction. Kulić and Schiessel predicted a *flipping-up-and-down* pathway of transition for the normal vector of a spool of DNA helically coiled onto a histone protein.[12] Such transition was not observed in this study. This finding suggests an important role played by the histone protein. For a DNA-histone spool under tension, the radius of the spool is restricted by the histone core. To pull a loop out of the spool inevitably induces a flipping-up-and-down movement of the spool. On the other hand, for a spool of DNA wrapped onto itself by multivalent counterions, a loop can be released gradually by decreasing the radius; therefore, the motion of the spool is more gentle and θ oscillates in a small range of angle, as seen in our case. This delicate difference of the dynamics between these two systems will be clarified more clearly in the future.

In summary, we have demonstrated that the loop-by-loop unfolding of a toroidal PE produces the stick-release pattern in FEC. We have shown how the internal structure of a toroidal condensate and its normal vector change during stretching. The results give deep insight of the elastic response and the structural transition of condensed DNA molecules being stretched.

Acknowledgment. This work is supported by the National Science Council (Grant No. NSC 97-2112-M-007-007-MY3). Computing resources are supported by the National Center for High-performance Computing. P.C.-L. acknowledges a graduate fellowship from the Taiwan Semiconductor Manufacturing Company.

References and Notes

(1) Vijayanathan, V.; Thomas, T.; Thomas, T. J. *Biochemistry* **2002**, *41*, 14085.
(2) (a) Smith, S. B.; Finzi, L.; Bustamante, C. *Science* **1992**, *258*, 1122. (b) Florin, E.-L.; Moy, V. T.; Gaub, H. E. *Science* **1994**, *264*, 415. (c) Simmons, R. M.; Finer, J. T.; Chu, S.; Spudich, J. A. *Biophys. J.* **1996**, *70*, 1813. (d) Bustamante, C.; Bryant, Z.; Smith, S. B. *Nature* **2003**, *421*, 423.
(3) Baumann, C. G.; Bloomfield, V. A.; Smith, S. B.; Bustamante, C.; Wang, M. D.; Block, S. M. *Biophys. J.* **2000**, *78*, 1965.
(4) Murayama, Y.; Sano, M. *J. Phys. Soc. Jpn.* **2001**, *70*, 345.
(5) Murayama, Y.; Sakamaki, Y.; Sano, M. *Phys. Rev. Lett.* **2003**, *90*, 018102.
(6) Marko, J. F.; Siggia, E. D. *Macromolecules* **1995**, *28*, 8759.
(7) (a) Bloomfield, V. A. *Curr. Opin. Struct. Biol.* **1996**, *6*, 334. (b) Hud, N. V.; Downing, K. H.; Balhorn, R. *Proc. Natl. Acad. Sci. U.S.A.* **1995**, *92*, 3581.
(8) Nguyen, T. T.; Rouzina, I.; Shklovskii, B. I. *J. Chem. Phys.* **2000**, *112*, 2562.
(9) Wada, H.; Murayama, Y.; Sano, M. *Phys. Rev. E* **2002**, *66*, 061912.
(10) Ueda, M.; Yoshikawa, K. *Phys. Rev. Lett.* **1996**, *77*, 2133.
(11) Wada, H.; Murayama, Y.; Sano, M. *Phys. Rev. E* **2005**, *72*, 041803.
(12) Kulić, I. M.; Schiessel, H. *Phys. Rev. Lett.* **2004**, *92*, 228101.
(13) Marenduzzo, D.; Martian, A.; Rosa, A.; Seno, A. *Eur. Phys. J. E* **2004**, *15*, 83.
(14) Lee, N.-K.; Thirumalai, D. *Biophys. J.* **2004**, *86*, 2641.
(15) Khan, M. O.; Chan, D. Y. C. *Macromolecules* **2005**, *38*, 3017.
(16) The simulations were run using a modified LAMMPS package. Refer to http://lammps.sandia.gov/ for LAMMPS.
(17) Stevens, M. J. *Biophys. J.* **2001**, *80*, 130.
(18) Wei, Y.-F.; Hsiao, P.-Y. *J. Chem. Phys.* **2007**, *127*, 064901.
(19) Tamashiro, M. N.; Schiessel, H. *Macromolecules.* **2000**, *33*, 5263.
(20) (a) Odijk, T. *Macromolecules* **1995**, *28*, 7016. (b) Wang, M. D.; Yin, H.; Landick, R.; Gelles, J.; Block, S. M. *Biophys. J.* **1997**, *72*, 1335.
(21) Hsiao, P.-Y. *Macromoleucles* **2006**, *39*, 7125.

MA802120B